We are IntechOpen, the world's leading publisher of Open Access books
Built by scientists, for scientists

6,900
Open access books available

186,000
International authors and editors

200M
Downloads

Our authors are among the

154
Countries delivered to

TOP 1%
most cited scientists

12.2%
Contributors from top 500 universities

CLARIVATE ANALYTICS
BOOK CITATION INDEX
INDEXED

WEB OF SCIENCE™

Selection of our books indexed in the Book Citation Index
in Web of Science™ Core Collection (BKCI)

Interested in publishing with us?
Contact book.department@intechopen.com

Density Functional Theory Studies of Catalytic Sites in Metal-Organic Frameworks

Siwarut Siwaipram, Sarawoot Impeng,
Philippe A. Bopp and Sareeya Bureekaew

Additional information is available at the end of the chapter

Abstract

Theoretical methods have become indispensable tools in many fields of chemistry and materials research. Metal-organic frameworks (MOFs) are porous materials; they have been intensively developed due to their diverse properties suitable for a wide range of applications. Theoretical approaches have thus been frequently employed toward the design and characterization of MOFs. We focus here in particular on theoretical studies of single-site catalytic reactions that occur inside the cavities of MOFs. The density functional method (DFT) has been the main approach used for such studies. We briefly review the uses of DFT to examine the catalytic reactions in MOFs. We note that DFT methods are versatile and can be made to work for different purposes such as, e.g., force-field development for molecular simulations. We shall, however, cover this field only very succinctly to put it into context with our main topic.

Keywords: theoretical chemistry, computational chemistry, quantum chemistry, density functional theory (DFT), metal-organic frameworks (MOF), catalysis, single-site catalytic reactions

1. Introduction

Experiments in chemistry aim primarily at understanding, or insight. These insights lead in turn to "innovation" and new technologies [1]. However, in many instances, such an insight cannot be obtained purely from current experiments. The required fundamental theory has been available for some time. The more recent development of computational methodologies and the dramatic increase in computer power made computational methods an additional

and competitive tool to describe chemical phenomena [2]. This field is broadly known as "modeling." In "molecular modeling," the premise is that the interatomic and intermolecular interactions can be known [3]. DFT has become the dominant tool for the purpose of determining such interactions [4]. In particular, in solid-state chemistry and physics, it has become increasingly popular since appropriate functionals and basis sets [5] were designed to provide a viable balance between the reliability of the numerical results and the computational costs.

Metal-organic frameworks (MOFs), also known as porous coordination polymers (PCPs) [6–8], are a class of hybrid organic-inorganic materials with high surface area, a permanent porosity with large internal pore volume and tunable pore sizes. They have a wide range of potential applications such as gas storage [9] and separation [10], catalysis [11], and many others [12–14]. MOFs are constructed by interlinking metal ions or, more generally, metal-containing units with organic moieties (carboxylates, azolates, imidazolates, pyridyl, etc.) through coordination bonds, thus creating crystalline frameworks. Due to the variety of the structural and chemical elements, some MOFs show unexpected characteristics, which sometimes cannot be fully assessed experimentally. Theoretical approaches have been intensively employed in this particular case to investigate the systems at the atomic level. Beyond the analysis of observed phenomena, the prediction of unknown attributes has been attempted.

In this book-chapter, we review and discuss the current status and challenges of DFT studies of MOFs. We focus in particular on aspects relevant to catalysis at the metal centers found in these structures.

2. DFT calculations on MOFs

One of the main issues of DFT calculations is that a compromise between the dependability of the results and computational costs must be found, especially for large and complex systems [15]. A primary issue is how to select a functional suitable for the investigated system [16]. Different functionals, based on different approximations, may give different (even opposite) results. It is thus important to choose the functionals wisely. No functional devised up to now has proven to be suitable for all systems. Therefore, the validation of any selected functional is crucial.

MOFs are crystalline materials with extended frameworks. This needs, in some instances, to be taken into account when, for catalytic applications of MOFs, DFT is used to investigate the reaction mechanism. The reaction enthalpy can be obtained approximately from the energy at 0 K by including a zero-point energy correction calculated from (possibly scaled) vibrational frequencies. To compute the entropy, harmonic or anharmonic low-frequency modes can be used. The temperature-dependent free and activation energies can be calculated by adding thermal enthalpic and entropic effects. The so-obtained free energies of reaction are used to calculate temperature-dependent equilibrium constants. Note that the kinetics of a reaction can also be investigated, e.g., by transition state theory (TST) [17]. However, this is beyond the scope of this chapter.

Since the properties of MOFs depend not only on their chemical composition but also their structures, atomistic structural characterization is essentials. Generally, the structure of a newly synthesized MOF is characterized by single-crystal X-ray diffraction (SC-XRD). If the

quality of the single crystals is not sufficient, the structure can be inferred from powder diffraction patterns [18] which often remains incomplete because of the complicated molecular system, large unit cell, and low symmetry. Molecular modeling methods must thus complement these experiments [19].

The periodic structure of an MOF can be studied by DFT: properties such as cell parameters and elastic properties can be obtained from periodic calculations. However, such calculations consume large amounts of computational resources due to the typically large unit cell of MOFs. Simple functionals such as local-density approximation (LDA) or generalized gradient approximations (GGA) are, however, often sufficient in this case [20]. Studying catalytic effects requires more advanced "hybrid" functionals, e.g., BP86 [21], B3-LYP [22], or M06 series [23].

Molecular mechanics (MM) is a much cheaper computational method to study large systems. The reliability of these calculations depends on the quality of the force fields used to describe the interactions between the atoms in the investigated system. Some high-accuracy force fields for MOFs, such as BTW-FF [24], MOF-FF [25], Quick-FF [26], and others [27, 28], were parametrized from DFT calculations. They were successfully used to determine and predict the periodic structures [29, 30], as well as to examine phase transformations [31–33], guest diffusion in the pores and other mechanical properties such as bulk moduli [34], elastic constants [35] and mechanical stability [36]. Note that MM calculations cannot describe electronic structures. Bond breaking and forming cannot be accounted for in such calculations. Thus, it is not possible to study reaction mechanisms using conventional MM methods [37].

In summary, for structurally well-defined and small enough systems, DFT calculations are a cogent approach especially in the field of localized catalytic reactions. We aim here to outline the suitability of DFT techniques to study catalysis in MOFs materials through examples from the recent literature.

3. Catalytic MOFs

MOFs have well-defined crystal structures with high concentrations of metal centers organized at topical distances, and large pore volumes between these centers. Even though MOFs are less able to withstand high temperatures compared to some other catalytic porous materials, their undeniable qualities such as large internal surface areas and uniform pore and cavity sizes make them attractive for various applications [38]. The pore size/shape in the framework can be tuned for selectivity for a particular reaction. In contrast, the small pore windows of other nanoporous materials, such as zeolites, commonly limit the catalytic transformation of large molecules [39].

In principle, various types of active sites can be incorporated into MOFs. Coordinatively unsaturated metal sites (CUSs) and functional groups on the organic linkers (usually acid/base sites) are the main catalytic sites. In addition, even though the MOF framework itself does not contain active sites, the catalytic reactivity can be enhanced by (a) postsynthetic functionalized modification [40] and (b) encapsulation of catalytic species [41]. The pore volume of MOFs is able to accommodate organic molecules, inorganic nanoparticles, metal complexes,

and enzymes to conduct catalytic reactions. Here, we focus only catalytic reactions taking place on one CUS.

It is because of these functionalities [39] that MOFs were originally proposed for applications in catalysis. From this point of view, one tends to focus on the design and synthesis of MOFs with large pore sizes. The purpose is to allow the reactant to diffuse easily into the framework reaching the catalytic centers. Suitable synthetic techniques make it possible to choose the linkers and the metal-containing nodes to construct MOF suitable for particular reaction. Such a well-designed MOF catalyst should be highly reactive, selective, and stable. In order to approach this goal, some understanding of the reaction mechanisms is essential. In many cases, the reactants and resulting products tend to be well localized, for a sufficiently long time, in the framework due to host-guest interaction. The catalytic site can thus often be separated from the framework and investigated independently, making it easier to follow the reaction mechanisms [42].

We focus in this brief overview, mostly through a series of examples, on such local analyses of the activity of single-site catalysts. Selected examples of work based on cluster, or truncated, models of reactions catalyzed by metal centers, metal substitutions, and deposited metal complexes are succinctly reviewed.

4. Catalytically reactive metal nodes

As mentioned above, MOFs are built up from metal ions or metal-containing clusters as the inorganic building node and organic ligands as linkers. In some MOFs, coordinatively unsaturated metal sites (CUSs) have a catalytic effect. The sites are spatially well separated and, ideally, structurally identical. Thus, to investigate the reaction mechanism with DFT methods, truncated structures can often be used to represent the entire MOFs.

4.1. Reactivity of coordinatively unsaturated metal sites

MOFs with CUSs provide identical active metal sites, which are spatially isolated from each another. The sites are structurally well-characterized, without coupling to their neighbors. In typical dense heterogeneous catalyst, the reaction takes place on the outer surface [43]. One way to enhance the catalytic effect is to increase the accessible surface area. In MOFs, reactions occur not only on the outer surface, easily accessible active sites inside the framework also contribute.

Maihom et al. investigated the epoxidations of ethylene over $Fe_3(BTC)_2$ (BTC = 1,3,5-benzenetricarboxylate) using N_2O as oxidant [44]. **A** truncated model $[Fe_2(H_2BTC)_4]$ (**Figure 1a**) was used. The reaction mechanism started with the N_2O decomposition over Fe to generate an active Fe-oxo moiety, requiring an activation energy of 23.7 kcal/mol. An ethylenoxy intermediate, and eventually, ethylene oxide, were obtained as final products rather than acetaldehyde (**Figure 1b**).

An investigation of the epoxidation of propylene using $Cu_3(BTC)_2$ and $Fe_3(BTC)_2$ was recently carried out by the same group [45]. As mentioned, truncated clusters, $[Cu_2(H_2BTC)_4]$ and $[Fe_2(H_2BTC)_4]$, are suitable for these calculations, carried out at the M06-L/6-31G(d,p) level. As expected, the calculations showed that $Fe_3(BTC)_2$ is more active than $Cu_3(BTC)_2$ due to a
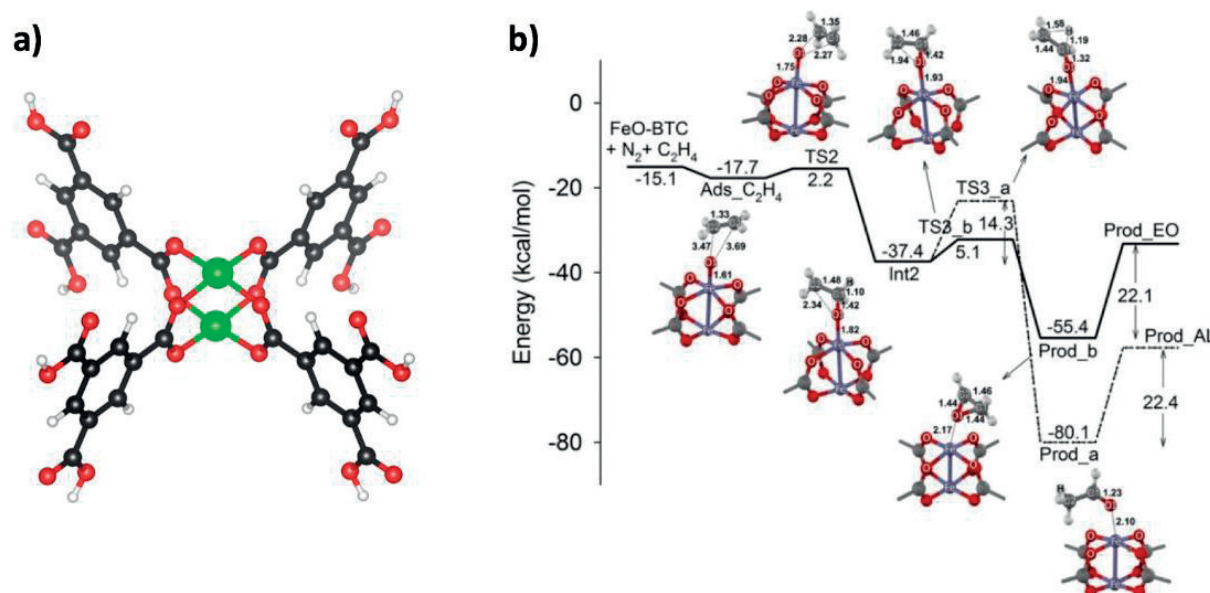
Figure 1. (a) Truncated model of $[Fe_2(H_2BTC)_4]$ and (b) energy profile of reactants, intermediates, and transition states involved in the formation of ethylene oxide (solid line) and the acetaldehyde (dash line) over the Fe paddle wheel. Adapted from Ref. [44] with permission of Wiley, copyright 2016.

larger charge transfer from the CUS to the oxidant O_2. It was found that the production of propylene oxide is favored over that of carbonylic products (propanal and acetone). Propanal and acetone were formed on the Fe-MOF cluster via the formation of a C━O bond. Then, the propyleneoxy intermediates and acetone are formed via a 1,2-hydride shift.

The M-MOF-74 series (M_2(DOBDC), where DOBDC = 2,5-dioxidoterephthalate and M = Mg, Ni, Co, Cu, and Zn) has been proposed as good catalysts for several reactions, owing to their reactive CUSs and large 1D channels, beneficial for the reactants' access to the active site. They are also thermally and chemically very stable [46–48]. Valvekens et al. [49] used MOF-74 with various metal ions, i.e., Mg (II), Ni (II), Co (II), Cu (II), and Zn (II) as Lewis acid catalysts to promote Knoevenagel condensations and Michael additions.

DFT calculations were performed on truncated models cut from the periodic geometries (**Figure 2**) optimized at the PBE-D2 level. The catalytic activities of M_2(DOBDC) systems with respect to the Knoevenagel condensation and Michael additions were examined. The calculations at the B3LYP level with a 6–31 g(d) basis showed that Ni-MOF-74 is the most active catalyst for both reactions. In addition, it was found that the phenolate groups coordinated with the CUSs substantially increase the catalytic performance. The phenolate oxygen proved to be a stronger base than the carboxylate oxygen, resulting in more acidic CUSs, enhancing the catalytic activity.

Llabrés i Xamena et al. [50] demonstrated that Cu(2-pymo)$_2$ and Co(PhIM)$_2$ (2-pymo and PhIM are 2-hydroxypyrimidinolat and phenylimidazolate, respectively) promote the aerobic oxidation reaction converting tetralin hydrocarbon to ketone and alcohol derivatives. The tetralin was first oxidized to hydroperoxides under oxygen condition and then decomposed to ketone and alcohol under the influence of the Lewis acid sites Cu(II) and Co(II). Ryan et al. [51] studied the mechanism of the hydroperoxide decomposition over three different complexes
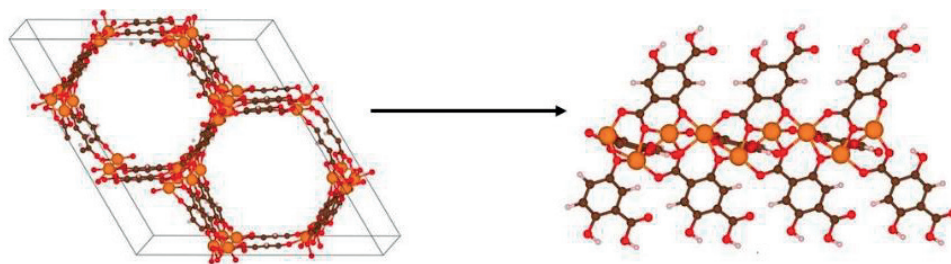
Figure 2. Periodic structure of M$_2$(DOBDC) optimized at the PBE-D2 level of theory (left), and the cluster model M$_9$(DOBDC)$_9$, truncated from the periodic structure (right). Adapted from Ref. [49] with permission of Elsevier, copyright 2014.

possessing copper or cobalt CUSs, i.e., Co(imidazolate)$_4$, Cu$_2$(2-hydroxypyrimidinolat)$_4$, and Cu$_2$(acetate)$_4$, as illustrated in **Figure 3**.

From DFT calculations (B3LYP/TZVP/6-31G(d,p)), the access of hydroperoxide to the CUSs of Cu$_2$(2-hydroxypyrimidinolat)$_4$ and of Co(imidazolate)$_4$ was found to be blocked by this bulky ligand. As a consequence, no decomposition of hydroperoxide was observed for the two systems. On the other hand, for Cu$_2$(acetate)$_4$, i.e., without the bulky ligands, the decomposition should occur. However, the calculations revealed that Cu$_2$(acetate)$_4$ was not active for the decomposition of tetralin. The energy barrier of the O—O bond cleavage over Cu$_2$(acetate)$_4$ (35.6–36.8 kcal/mol) was almost identical with that of the cleavage in the gas phase without catalyst (36.0–36.7 kcal/mol). The external surface was then considered as the active sites.

A complex consisting of Cu coordinated by three organic linkers and one water molecule was modeled representing the edge or outer surface of the framework (**Figure 4a**). The energy barrier of the hydroperoxide decomposition on the new model complex decreased to 25.3 kcal/mol, which was considerably lower than the value of the gas-phase reaction without MOFs as shown in **Figure 4b**.

Vanadium-based MIL-47(V), [VO(BDC)] (BDC = benzene-1,4-dicarboxylate), is an active catalyst for the liquid-phase cyclohexene oxidation-reaction using tert-butyl hydroperoxide (TBHP) as an oxidant [52]. MIL-47(V) is built up from linear V-(μ_2-O)-V chains interconnected
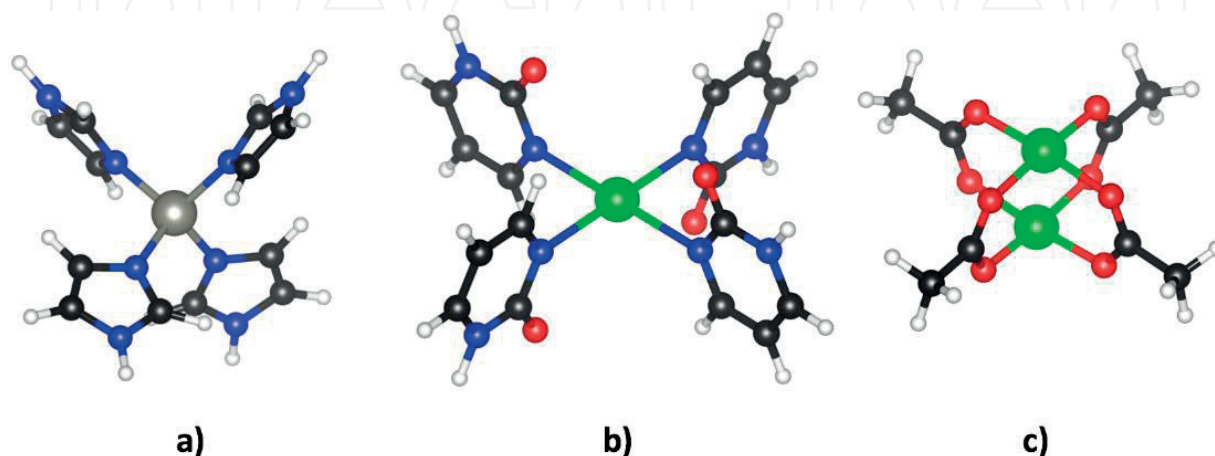
Figure 3. The metal cluster models taken from (a) Co(imidazolate)$_4$, (b) Cu$_2$(2-hydroxypyrimidinolat)$_4$, and (c) Cu$_2$(acetate)$_4$.
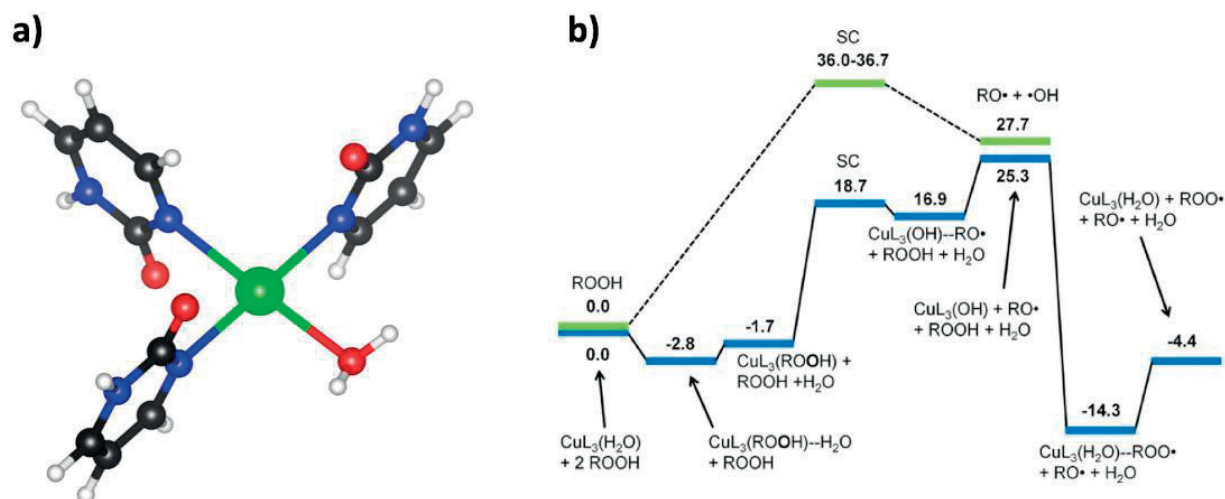
Figure 4. (a) Model of a cluster representing the exterior of a Cu_2(2-hydroxypyrimidinolat)$_3$ with one water molecule, (b) Gibbs free energy along the reaction coordinate for the proposed reaction cycle over the Cu_2(2-hydroxypyrimidinolat)$_3$ with one water molecule (blue) and oxygen—oxygen bond cleavage without catalyst (green). All energies are in kcal/mol. Figure adapted from Ref. [51] with permission of Elsevier, copyright 2012.

by terephthalate linkers to form a 3D framework possessing 1D rhombic channels. Each V(IV)-center in this chain coordinates to six oxygen atoms—four from carboxylate and two from μ_2O. Typically, MIL-47(V) does not provide CUSs. However, CUSs can be created from structural defects obtained by partially breaking the V—O_{COO} bonds and from the hydrolysis of the V—O_{COO} bonds.

The main products of the cyclohexene oxidation reaction are cyclohexene oxide, cyclohexane-1,2-diol, tert-butyl-2-cyclohexenyl-1-peroxide, and 2-cyclohexen-1-one with a conversion of about 80%. It was found that the catalytic performance of MIL-47(V) was comparable with that of typical homogeneous catalyst, VO(acac)$_2$. Note that no leaching of V(IV) was observed when the oxidant was dissolved in the solution. The structures of the MIL-47(V) were maintained intact until the end of reaction. Leus and Vandichel et al. [52] proposed a reaction pathway from DFT calculations on finite clusters of MIL-47(V) (**Figure 5**).

The results were in good agreement with EPR and NMR measurement that are interpreted in terms of the existence of (at least) two different catalytic pathways, described as the "direct" and "radical" pathways [52]. The first step of both pathways was the formation of a vanadium hydroperoxide species from TBHP. For the direct pathway, cyclohexene was directly converted to cyclohexene oxide, while the oxidation state of vanadium (V(IV)) did not change during the reaction. In the case of the radical pathway, V(IV) was oxidized to V(V), which further reacted with the oxidant TBHP to give an active species of the cyclohexene epoxidation. Finally, the catalyst was regenerated by interacting with TBHP again. At the B3LYP-D3 and 311 + g(3df,2p) level of theory, the reaction free energy for epoxidation reaction was 37 kJ/mol for the more favorable radical route.

Moreover, Matthias et al. [53] studied the cyclohexene oxidation using MIL-47(V)-functionalized linkers (with the functional groups —OH, —F, —Cl, —Br, —CH$_3$, and —NH$_2$) by means of experimental and theoretical works. Different catalytic conversions were observed depending on the functionalization of the linkers. DFT calculations on truncated clusters of MIL-47(V) and its derivatives were performed as in the abovementioned example for the radical
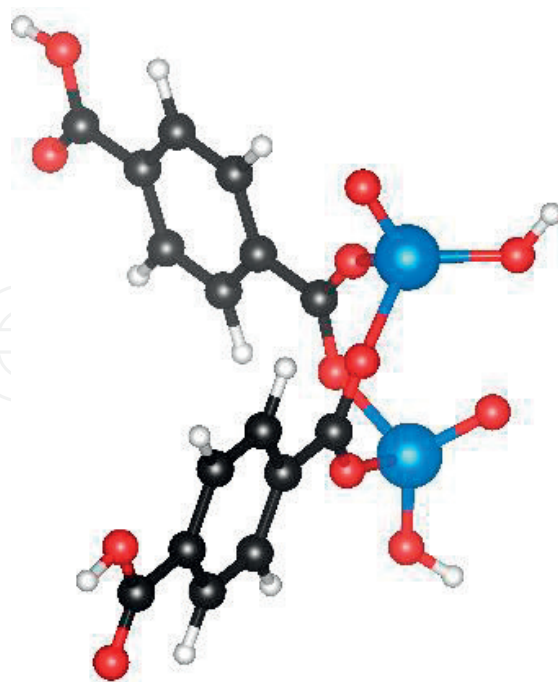
Figure 5. Simulated model of V-MIL-47.

pathway. The results showed that, compared to the parent MIL-47(V), the catalytic efficiency significantly increased due to the functional groups. Among these, the ▬OH-functionalized structure showed the largest improvement (lowest activation energy), which was in good agreement with the experimental results. This is because of a strong hydrogen bond between the ▬OH and the alkylperoxo group possibly stabilizing the transition state.

4.2. Reactivity of substituted metal centers as single-site catalysts

Partial substitution of metal ions while maintaining the structural integrity and the porosity is a promising strategy enabling some otherwise inactive MOFs to show a catalytic activity [54]. The metal substitution usually involves the cleavage and regeneration of coordination bonds between metal ions and organic ligands. The atomic-level understanding of this process is difficult, making room for molecular modeling. Here, we show examples of theoretical studies on the catalytic activity of metal-substituted MOFs.

Xiao et al. [55] reported the oxidation reaction of ethane to ethanol over magnesium-diluted $Fe_{0.1}Mg_{1.9}(DOBDC)$, MOF-74, in which 5% of the redox-inactive Mg(II) were substituted by the active Fe(II). This framework provides wide hexagonal channels beneficial for an easy access of the reactants to the site-isolated open Fe-CUSs. Nitrous oxide (N_2O) was used as the oxidant, generating highly reactive Fe(IV)-oxo intermediates, which could further activate strong C▬H bonds of alkanes, yielding ethanol and acetaldehyde. Owing to the short lifetime of Fe(IV)-oxo, it could neither be isolated nor characterized by conventional experiments.

Shortly afterward, Verma el al. [56] applied DFT calculations to confirm whether the Fe(IV)-oxo species are formed and act as active centers for ethane hydroxylation to ethanol. They modeled the Fe sites in magnesium-diluted $Fe_2(DOBDC)$ by replacing 1 Mg atom with Fe atom in cluster models comprising 88 atoms of Mg-MOF-74. The oxidation of ethane to ethanol over

this magnesium-diluted MOFs using N_2O as oxidant was proposed to proceed via a two-step consecutive reaction (**Figure 6**): the formation of the Fe(IV)-oxo unit via N_2O decomposition and the hydroxylation of ethane to ethanol over the Fe(IV)-oxo complex. It is found that the first step is the rate-determining step with an activation energy of 82 kJ/mol. Compared to the uncatalyzed reaction, where nitrous oxide directly oxidizes the ethane to ethanol, it was found that the reaction requires an activation barrier of 280 kJ/mol. This suggests that the Fe(IV)-oxo species is indeed an active center for the oxidation of ethane to ethanol.

In the meantime, Hirrao et al. [57] also carried out combined quantum and molecular mechanics (QM/MM) calculations for the hydroxylation of ethane, in analogy to Mg-MOF-74. This methodology treats the active site by QM and the rest of the system is treated by MM. The accuracy of QM/MM methods certainly depends on the choice of the QM theory level and the set of MM parameters, also on the treatment of electrostatics at the interface between the QM and MM regions. One of three Mg(II) ions was substituted by Fe(II) in the QM region, as in the model suggested by Verma et al. [56]. In the ONIOM [58] scheme, the MM region was treated at the B3LYP/[SDD(Fe),6-31G(d)(others)] level while the UFF interaction model [59] was used for the MM region. The 6–311 + G(df,p) basis set was used for single-point reference calculations. This work also suggested that the spin state (S = 2) of the Fe(IV)-oxo species does not change during the reaction.

Interestingly, Liao et al. [60] then improved based on Verma et al. model [56] the understanding on the activity of Fe open sites for the oxidation of ethane reaction. They studied MOF-74 with different linkers, in particular, $—CH_3$, NH_2, $—COOH$, $—CN$, $—OH$, $—OCH_3$, $—N(CH_3)_2$,
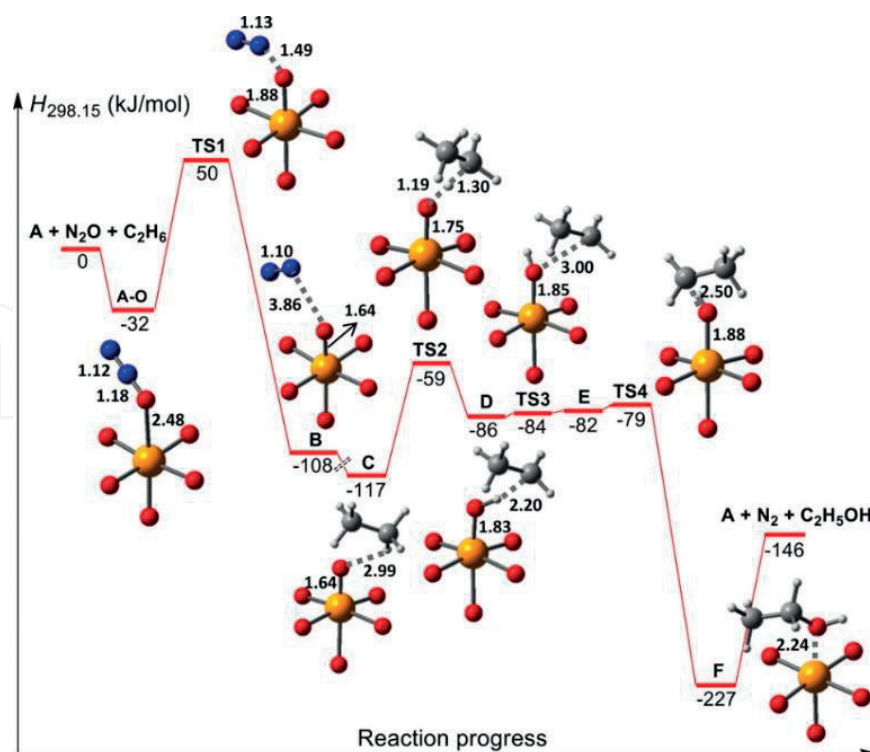
Figure 6. Enthalpy profile, $\Delta H_{298.15}$ (in kJ/mol), for the intermediates and transition states of the catalytic cycle. The key bond distances are given in Å (color code: orange = Fe, red = O, blue = N, gray = C, and white = H). Reproduced from Ref. [56] with permission of the American Chemical Society, copyright 2015.

and 4-pyridyl functionalized groups on different linkers such as using methanol, pyridine, formate, benzoate anion, and the imidazole anion. The authors concluded that the population of the d-orbital was significantly influenced by the coordination ligand field. The 3d orbital energy of Fe correlated with the electron-donating strength of the functional groups on the linkers. The results reveal that linkers with ━NH$_2$ groups reduce the enthalpic barrier for the most endothermic step in the ethane oxidation pathway. This study illustrates the use of simple models to understand complicated and computationally intensive systems. The activity of CUSs thus might be optimized by selecting suitable ligand environments, which might be useful for upgrading certain hydrocarbon process.

The design of Fe(IV)-oxo complexes in MOFs was further reported by Impeng et al. [61]. In this work, we demonstrated the possibility of designing Fe-oxo complexes in MOFs for the activation of alkane C━H bond by incorporating an Fe ion into a Zn-based cluster derived from Zn$_4$O(BDC)$_6$, known as MOF-5 [62], and generating the Fe-O unit through N$_2$O dissociation on an Fe-substituted Zn-based cluster (Fe-Zn$_3$O(pyrazole)$_6$). The calculations with B3LYP-D3 showed that both steps are feasible and that the catalytic activity of Fe-Zn$_3$O(pyrazole)$_6$ for N$_2$O decomposition is on a par with the Fe sites in magnesium-diluted Fe$_2$(DOBDC). Concerning ethane C━H bond activation, in addition to σ and π pathways on triplet and quintet surfaces, an alternative unusual pathway, called δ, is also observed on the triplet surface. The σ pathway on the quintet surface (TS$_\sigma^5$) has the lowest activation energy owing to less steric hindrance and favorable d-d interactions on the Fe active site at the transition state, as illustrated in **Figure 7**.
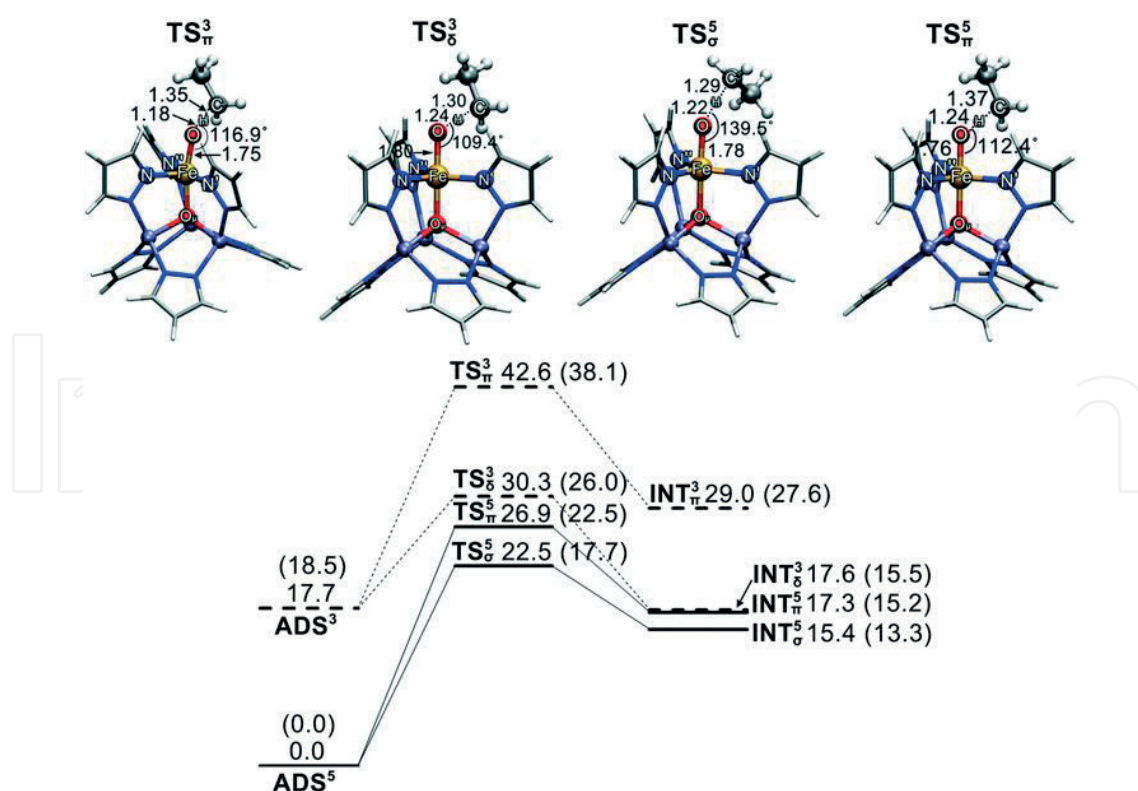
Figure 7. Reaction profile for ethane C━H bond activation over the FeO-Zn$_3$O(pyrazole)$_6$ cluster. The inserted numbers are the relative energies ΔE, together with the enthalpies ΔH$_{298K}$ in parentheses. Energies are given in kcal/mol and distances are expressed in Å. The notations ADS, TS, and INT refer to the adsorption, transition, and intermediate steps, respectively. Superscripts 3 and 5 refer to the triplet and quintet spin states, respectively.

## 5. Reactivity of metal nodes deposited as single-site catalysts

In this section, we discuss systems possessing metal-complexes/ions anchored on the inorganic building nodes of the framework, which can be achieved by postsynthetic techniques such as metalation [63], cation exchange [64], or atomic layer deposition [65]. Zr-based MOFs consist of Zr_6O_8 as a primary node linked with carboxylate linkers. The Zr_6O_8 nodes connected by 12 linkers result in the UiO-66 series, while the partial connection with 8 and 6 carboxylates produces NU-1000 and MOF-808, respectively. The catalytic reactivity can be enhanced through such modifications. This was often employed for Zr-based MOFs, which are remarkable because of their appealing chemical and thermal stability [40]. Well-known Zr-based MOFs such as MOF-808 $[Zr_6(\mu_3\text{-}O)_4(\mu_3\text{-}OH)_4(OH)_6(H_2O)_6(BTC)_2]$, NU-1000 $[Zr_6(\mu_3\text{-}O)_4(\mu_3\text{-}OH)_4(OH)_4(H_2O)_4(TBAPy)_2]$ (TBAPy = tetratopic 1,3,6,8-tetrakis(p-benzoate)pyrene) and UiO-66, known as NU-1000 and $[Zr_6(\mu_3\text{-}O)_4(\mu_3\text{-}OH)_4(BDC)_6]$, known as UiO-66 have been studied intensively [66, 67].

Ortuño et al. [68] reported on a computational screening of the first row of divalent transition metals (i.e., Fe(II), Co(II), Ni(II), Cu(II), and Zn(II)) supported on NU-1000 (**Figure 8**) for acceptorless alcohol dehydrogenation. The author proposed the reaction taking place via a three-step reaction mechanism, composed of (i) a proton transfer, (ii) β-hydride elimination, and (iii) H▬H bond formation. The Fe(II), Co(II), and Ni(II) complexes, consistent with weak-field oxide ligands, had high-spin ground electronic states as quintet, quartet, and triplet, respectively. The Cu(II) and Zn(II) species were predicted to have doublet and singlet ground states, respectively. It was found that the Co(II) and Ni(II) supported NU-1000 were the two most promising catalysts for the acceptorless alcohol dehydrogenation with an activation free energy of 28.5 and 26.5 kcal/mol, respectively.

Later, the same group also studied Ni(II) and Co(II) deposited on Zr-NU-1000 as a catalyst for ethylene dimerization, which converts ethylene to 1-butene and 2-butene [69]. For the structure optimization, the DFT level of theory (M06-L) and def2-TZVPP basis set were employed, whereas complete active space self-consistent field (CASSCF) and second-order perturbation theory (CASPT2) were used for the electronic structure characterization of the reactive species. The NU-1000 models were used as the same as in the previous example (**Figure 8**). The grafted Ni and Co were terminated with active ▬OH and ▬OH_2 groups.

The Cossee-Arlman mechanism was found as the energetically preferable pathway. Ethylene insertion into the existing metal-ethyl bond was the rate-determining step. Concerning the spin state of the two catalysts, the Co(II) species can have doublet or quartet states and the Ni(II) can have singlet or triplet states. Based on these calculations, Ni(II)-modified NU-1000 (with an activation energy of 15.6 kcal/mol) presents a greater reactivity than the Co(II)-modified system (with an activation energy of 24.1 kcal/mol) for the ethylene insertion into the metal-carbon bond. The energetics of ethylene dimerization for the Ni(II) and Co(II) complexes are shown in **Figure 9**. From the most relevant CASSCF molecular orbitals (MOs), the 3d orbitals of the low-spin Ni(II) complex hybridized with the 2p orbitals of the active carbon atom because of the empty fifth orbital. In contrast to the high-spin Co(II) complex, the degree of hybridization in the Ni-case is less able to stabilize the TS structure due to the half-filled 3d orbital, leading to a lower catalytic activity.
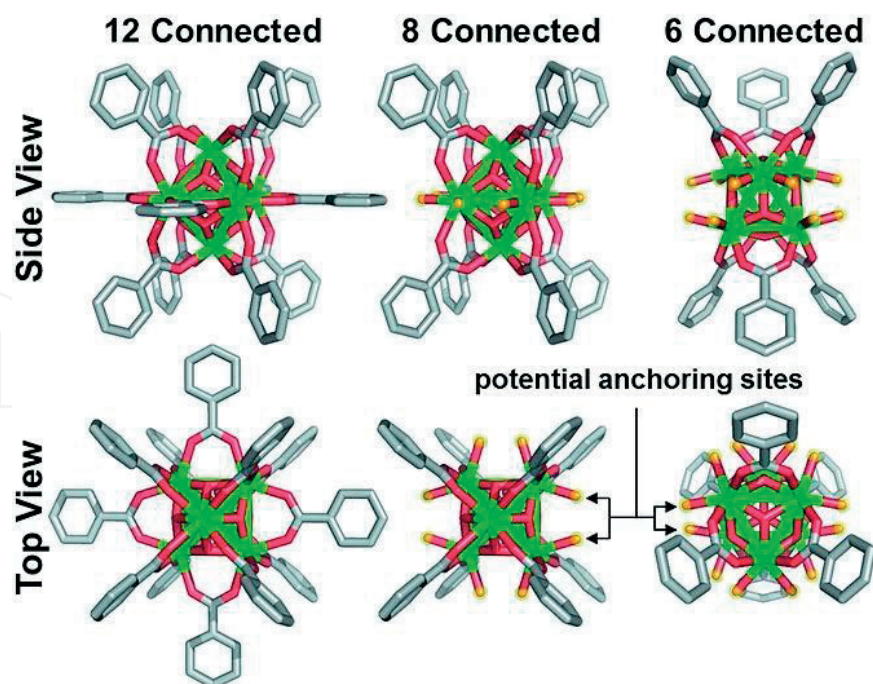
Figure 8. The "top" and "side" views of a 12-, 8-, and 6-connected Zr_6 oxide node. The arrows indicate the unsaturated 8- and 6-connected nodes, which have potential anchoring points. Reproduced from Ref. [66] with permission of Wiley, copyright 2016.

The oxidative dehydrogenation mechanism of propane on an active Co(II)-oxygen cluster anchored on the inorganic node of Zr-NU-1000 [70] was also explored by DFT with the M06-L functional and def2-TZVPP. A highly selective propane dehydrogenation at low temperature (230°C) has been found in experiments. Li et al. [70] found a computed propene formation
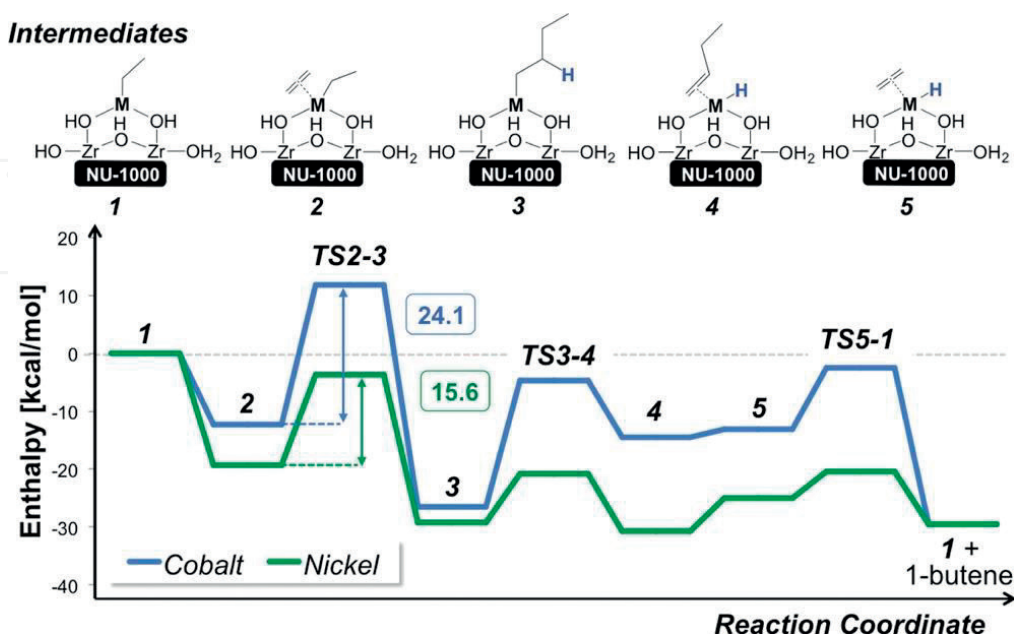
Figure 9. Reaction coordinate and calculated enthalpy $\Delta H_{298.15K}$ for stationary points along the reaction coordinates for ethylene dimerization catalyzed by M(II)-NU-1000 (M = Co and Ni). Reproduced from Ref. [69] with permission of the American Chemical Society, copyright 2016.
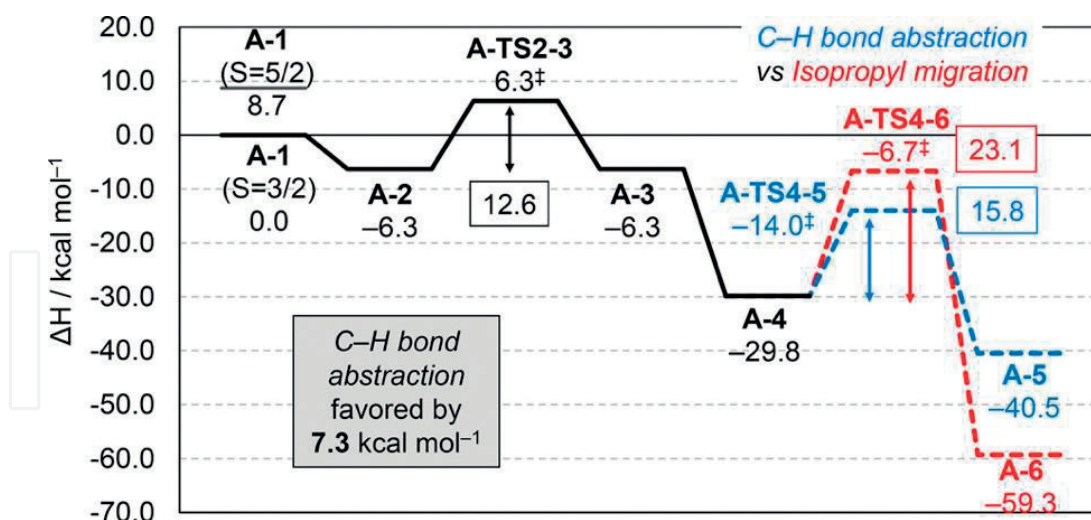
Figure 10. Computed enthalpies, ΔH_{503K} (kcal/mol), for propane oxidative dehydrogenation. Reproduced from Ref. [70] with permission of the American Chemical Society, copyright 2017.

in line with experimental results. DFT cluster calculations allowed to study the reaction and showed the influence on the reaction of adding Co(II) cations as a secondary metal. The computed enthalpies for the equilibrium structures are shown in **Figure 10**.

In more detail, the reactive Co(III)—O· moiety was generated by the catalyst regeneration reaction with O_2 having a strong interaction with the propane molecules, promotes the propane dehydrogenation, and forms isopropyl at the Co(III) active site. The abstraction of the terminal C-H bond by the Co(III)—O· intermediate is the rate-determining step, yielding
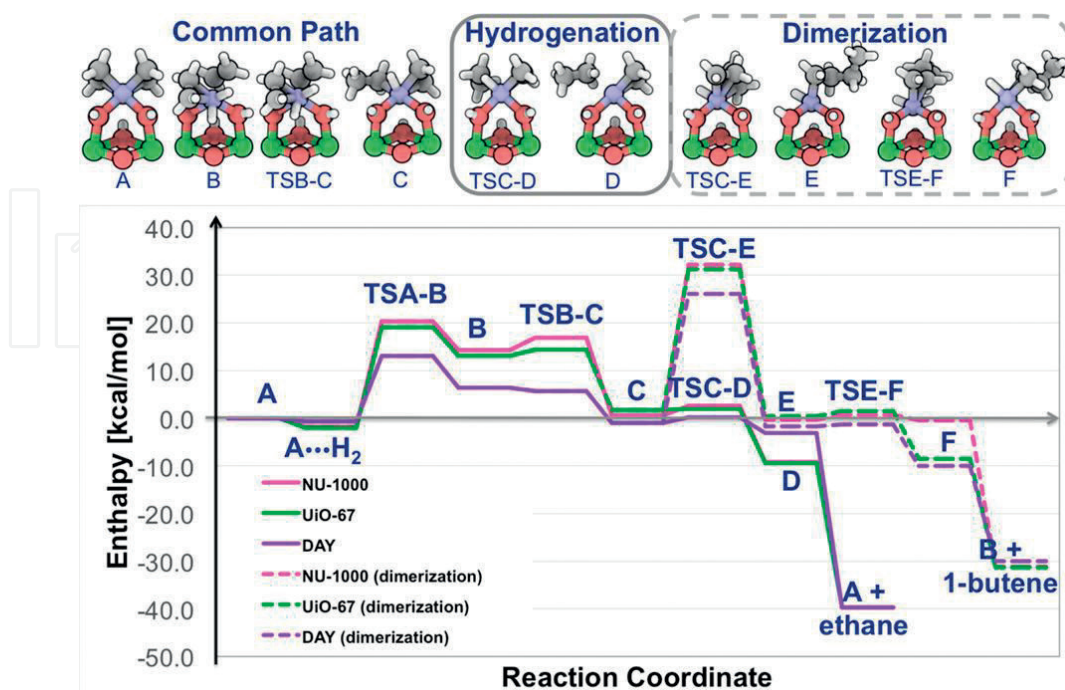
Figure 11. Calculated enthalpy, $\Delta H_{298.15K}$ (kcal/mol), for ethylene hydrogenation to ethane and dimerization to 1-butene catalyzed by supported metal complexes initially present as $Rh(C_2H_4)_2$ on NU-1000, UiO-67, or DAY zeolites. Reproduced from Ref. [71] with permission of the American Chemical Society, copyright 2017.

Co(II)━OH and isopropyl radicals, which are converted into propene. The energy required for the H abstraction producing propene (15.8 kcal/mol) was significantly lower than that for the isopropyl migration (23.1 kcal/mol), the propene formation path is thus preferable.

Gates et al. [71] showed that Rh(I) and Ir(I) diethylene complexes can be anchored on the Zr-NU-1000, Hf-NU-1000, and Zr-UiO-67 to catalyze ethylene hydrogenation and dimerization. They also used DAY zeolite as supporting material to compare the catalytic performance. DFT calculations with M06-L and def2-TZVPP were employed. The optimized geometries were in good agreement with the data analyzed from IR spectra and X-ray absorption fine structure (EXAFS) results. The ethylene insertion to the ethyl━Rh bond (rate-determining step) significantly depended on the nature of the supporting MOF. The catalytic activity was compared between Zr- and Hf-nodes and DAY zeolites. The calculated enthalpies for the ethylene hydrogenation and dimerization were shown in **Figure 11**. The calculations reveal a lower energy barrier of the DAY zeolite as supporting material than Zr-NU-1000, Hf-NU-1000, and Zr-UiO-67 for the hydrogenation and dimerization. This is opposite to the experiments which show a better catalytic activity of the DAY zeolite than the MOFs materials. The authors proposed that this might be because of the spillover effect rather than a direct electronic effect on the Rh(I) complex.

6. Outlook

We focus in this brief overview on theoretical studies of the catalytic activity of single-site catalytic MOFs. DFT-based approaches can provide a detailed, if only local, description of the chemistry occurring in various environments encountered in such MOFs. This not only helps in the interpretation of experiment data; the abilities of DFT calculations are a crucial characterization method toward a deeper molecular perspective. This technique is now powerful and reliable enough to predict and guide the synthesis of materials.

There are, however, several problems which need to be overcome:

  I. To find a link between a predicted structure and its syntheses still a challenge.

 II. Sometime nonlocal phenomena such as a stimulus-responsive behavior of the catalytic site itself must be taken into account. Many works[ref] attempt to simulate larger models in order to describe such systems. This seems to require improved methodologies to limit the computational requirements.

III. The functionals: Since there is no "universal functional" DFT must be always used with a lot of caution. A lot of experience has been accumulated on the suitability of various approximations to investigate MOFs. Yet new, and costly, validations are still required whenever a "new" system is to be studied.

IV. Last but not least, in some cases, a local view as described in this chapter may not be sufficient to catch the main features of a particular process. The overall outcome of the process under study may depend on many factors, in the worst case, none of which dominant. Various "local views" that may have been obtained could be combined as building blocks (e.g., by understanding the molecular motions between "sites"). This remains largely a task for theoretical improvements in the future.

Acknowledgements

Conflicts of interest

There are no conflicts to declare.

Author details

Siwarut Siwaipram[1], Sarawoot Impeng[2], Philippe A. Bopp[1,3] and Sareeya Bureekaew[1*]

*Address all correspondence to: sareeya.b@vistec.ac.th

1 Department of Energy Science and Engineering (ESE), Vidyasirimedhi Institute of Science and Technology (VISTEC), Rayong, Thailand

2 National Nanotechnology Center (NANOTEC), National Science and Technology Development Agency, Pathumthani, Thailand

3 Department of Molecular Science and Engineering (MSE), Vidyasirimedhi Institute of Science and Technology (VISTEC), Rayong, Thailand

References

[1] Anastas PT, Kirchhoff MM. Origins, current status, and future challenges of green chemistry. Accounts of Chemical Research. 2002;**35**(9):686-694. DOI: 10.1021/ar010065m

[2] Law AL. Simulation Modeling and Analysis. Vol. 2. New York: McGraw. McGraw-Hill New York; 2007. Retrieved from https://www.researchgate.net/

[3] Whitehead TL. Molecular modeling: Basic principles and applications, 2nd Edition (Hans-Dieter Höltje, Wolfgang Sippl, Didier Rognan, and Gerd Folkers). Journal of Chemical Education. 2006;**83**(6):851. DOI: 10.1021/ed083p851

[4] Becke AD. Density-functional thermochemistry. III. The role of exact exchange. The Journal of Chemical Physics. 1993;**98**(7):5648-5652. DOI: 10.1063/1.464913

[5] Pople JA, Gill PMW, Johnson BG. Kohn-Sham density-functional theory within a finite basis set. Chemical Physics Letters. 1992;**199**(6):557-560. DOI: 10.1016/0009-2614(92)85009-y

[6] Furukawa H, Cordova KE, O'Keeffe M, Yaghi OM. The chemistry and applications of metal-organic frameworks. Science. 2013;**341**(6149):123044-0-123044-12. DOI: 10.1126/science.1230444

[7] Férey G. Hybrid porous solids: Past, present, future. Chemical Society Reviews. 2008;**37**(1):191-214. DOI: 10.1039/b618320b

[8] Kitagawa S, Matsuda R. Chemistry of coordination space of porous coordination polymers. Coordination Chemistry Reviews. 2007;**251**(21-24):2490-2509. DOI: 10.1016/j.ccr.2007.07.009

[9] Murray LJ, Dincă M, Long JR. Hydrogen storage in metal-organic frameworks. Chemical Society Reviews. 2009;**38**(5):1294-1314. DOI: 10.1039/b802256a

[10] Li J-R, Kuppler RJ, Zhou H-C. Selective gas adsorption and separation in metal-organic frameworks. Chemical Society Reviews. 2009;**38**(5):1477-1504. DOI: 10.1039/b802426j

[11] Rogge SMJ, Bavykina A, Hajek J, Garcia H, Olivos-Suarez AI, Sepúlveda-Escribano A, et al. Metal-organic and covalent organic frameworks as single-site catalysts. Chemical Society Reviews. 2017;**46**(11):3134-3184. DOI: 10.1039/c7cs00033b

[12] Horcajada P, Serre C, Vallet-Regí M, Sebban M, Taulelle F, Férey G. Metal-organic frameworks as efficient materials for drug delivery. Angewandte Chemie. 2006;**118**(36):6120-6124. DOI: 10.1002/anie.200601878

[13] Horcajada P, Gref R, Baati T, Allan PK, Maurin G, Couvreur P, et al. Metal-organic frameworks in biomedicine. Chemical Reviews. 2012;**112**(2):1232-1268. DOI: 10.1021/cr200256v

[14] Hu Z, Deibert BJ, Li J. Luminescent metal-organic frameworks for chemical sensing and explosive detection. Chemical Society Reviews. 2014;**43**(16):5815-5840. DOI: 10.1039/C4CS00010B

[15] Sholl D, Steckel JA. Density Functional Theory: A Practical Introduction. John Wiley & Sons; 2009. pp. 1-33. DOI: 10.1002/anie.200905551

[16] Mattsson AE, Schultz PA, Desjarlais MP, Mattsson TR, Leung K. Designing meaningful density functional theory calculations in materials science—A primer. Modelling and Simulation in Materials Science and Engineering. 2004;**13**(1):R1. DOI: 10.1088/0965-0393/13/1/R01

[17] Steinfeld JI, Francisco JS, Hase WL. Chemical Kinetics and Dynamics. Vol. 3. New Jersey: Prentice Hall Englewood Cliffs; 1989. Retrieved from: http://www.academia.edu/

[18] Price SL. From crystal structure prediction to polymorph prediction: Interpreting the crystal energy landscape. Physical Chemistry Chemical Physics. 2008;**10**(15):1996-2009. DOI: 10.1039/b719351c

[19] Mellot-Draznieks C. Role of computer simulations in structure prediction and structure determination: From molecular compounds to hybrid frameworks. Journal of Materials Chemistry. 2007;**17**(41):4348-4358. DOI: 10.1039/B702516P

[20] Kohn W, Becke AD, Parr RG. Density functional theory of electronic structure. The Journal of Physical Chemistry. 1996;**100**(31):12974-12980. DOI: 10.1021/jp960669l

[21] Becke AD. Density-functional exchange-energy approximation with correct asymptotic behavior. Physical Review A. 1988;**38**(6):3098-3100. DOI: 10.1103/PhysRevA.38.3098

[22] Lee C, Yang W, Parr RG. Development of the Colle-Salvetti correlation-energy formula into a functional of the electron density. Physical Review B. 1988;**37**(2):785-789. DOI: 10.1103/PhysRevB.37.785

[23] Zhao Y, Truhlar DG. The M06 suite of density functionals for main group thermochemistry, thermochemical kinetics, noncovalent interactions, excited states, and transition elements: Two new functionals and systematic testing of four M06-class functionals and 12 other functionals. Theoretical Chemistry Accounts. 2008;**120**(1):215-241. DOI: 10.1007/s00214-007-0310-x

[24] Bristow JK, Tiana D, Walsh A. Transferable force field for metal-organic frameworks from first-principles: BTW-FF. Journal of Chemical Theory and Computation. 2014;**10**(10):4644-4652. DOI: 10.1021/ct500515h

[25] Bureekaew S, Amirjalayer S, Tafipolsky M, Spickermann C, Roy TK, Schmid R. MOF-FF-A flexible first-principles derived force field for metal-organic frameworks. Physica Status Solidi. 2013;**250**(6):1128-1141. DOI: 10.1002/pssb.201248460

[26] Vanduyfhuys L, Vandenbrande S, Verstraelen T, Schmid R, Waroquier M, Van Speybroeck V. QuickFF: A program for a quick and easy derivation of force fields for metal-organic frameworks from ab initio input. Journal of Computational Chemistry. 2015;**36**(13): 1015-1027. DOI: 10.1002/jcc.23877

[27] Coupry DE, Addicoat MA, Heine T. Extension of the universal force field for metal-organic frameworks. Journal of Chemical Theory and Computation. 2016;**12**(10): 5215-5225. DOI: 10.1021/acs.jctc.6b00664

[28] Fang H, Demir H, Kamakoti P, Sholl DS. Recent developments in first-principles force fields for molecules in nanoporous materials. Journal of Materials Chemistry A. 2014;**2**(2):274-291. DOI: 10.1039/C3TA13073H

[29] Impeng S, Cedeno R, Dürholt JP, Schmid R, Bureekaew S. Computational structure prediction of (4, 4)-connected copper paddle-wheel-based MOFs: Influence of ligand functionalization on the topological preference. Crystal Growth & Design. 2018;**18**(5): 2699-2706. DOI: 10.1021/acs.cgd.8b00238

[30] Bureekaew S, Balwani V, Amirjalayer S, Schmid R. Isoreticular isomerism in 4, 4-connected paddle-wheel metal-organic frameworks: Structural prediction by the reverse topological approach. CrystEngComm. 2015;**17**(2):344-352. DOI: 10.1039/C4CE01574F

[31] Alaghemandi M, Schmid R. Model study of thermoresponsive behavior of metal-organic frameworks modulated by linker functionalization. Journal of Physical Chemistry C. 2016;**120**(12):6835-6841. DOI: 10.1021/acs.jpcc.5b12331

[32] Wieme J, Vanduyfhuys L, Rogge SMJ, Waroquier M, Van Speybroeck V. Exploring the flexibility of MIL-47 (V)-type materials using force field molecular dynamics simulations. Journal of Physical Chemistry C. 2016;**120**(27):14934-14947. DOI: 10.1021/acs.jpcc.6b04422

[33] Evans JD, Bocquet L, Coudert FX. Origins of negative gas adsorption. Chem. 2016;**1**(6): 873-886. DOI: 10.1016/j.chempr.2016.11.004

[34] Boyd PG, Moosavi SM, Witman M, Smit B. Force-field prediction of materials properties in metal-organic frameworks. Journal of Physical Chemistry Letters. 2017;**8**(2):357-363. DOI: 10.1021/acs.jpclett.6b02532

[35] Ortiz AU, Boutin A, Fuchs AH, Coudert F-X. Metal-organic frameworks with wine-rack motif: What determines their flexibility and elastic properties? The Journal of Chemical Physics. 2013;**138**(17):174703. DOI: 10.1063/1.4802770

[36] Rogge SMJ, Wieme J, Vanduyfhuys L, Vandenbrande S, Maurin G, Verstraelen T, et al. Thermodynamic insight in the high-pressure behavior of UiO-66: Effect of linker defects and linker expansion. Chemistry of Materials. 2016;**28**(16):5721-5732. DOI: 10.1021/acs. chemmater.6b01956

[37] Van Duin ACT, Dasgupta S, Lorant F, Goddard WA. ReaxFF: A reactive force field for hydrocarbons. The Journal of Physical Chemistry. A. 2001;**105**(41):9396-9409. DOI: 10.1021/jp004368u

[38] Howarth AJ, Liu Y, Li P, Li Z, Wang TC, Hupp JT, et al. Chemical, thermal and mechanical stabilities of metal-organic frameworks. Nature Reviews Materials. 2016;**1**(3):15018. DOI: 10.1038/natrevmats.2015.18

[39] Kitagawa S, Kitaura R, Noro S. Functional porous coordination polymers. Angewandte Chemie, International Edition. 2004;**43**(18):2334-2375. DOI: 10.1002/anie.200300610

[40] Cohen SM. Postsynthetic methods for the functionalization of metal-organic frameworks. Chemical Reviews. 2011;**112**(2):970-1000. DOI: 10.1021/cr200179u

[41] Cui Y, Li B, He H, Zhou W, Chen B, Qian G. Metal-organic frameworks as platforms for functional materials. Accounts of Chemical Research. 2016;**49**(3):483-493. DOI: 10.1021/ acs.accounts.5b00530

[42] Liu J, Chen L, Cui H, Zhang J, Zhang L, Su CY. Applications of metal-organic frameworks in heterogeneous supramolecular catalysis. Chemical Society Reviews. 2014;**43**(16): 6011-6061. DOI: 10.1039/C4CS00094C

[43] Thomas JM, Raja R, Lewis DW. Single-site heterogeneous catalysts. Angewandte Chemie, International Edition. 2005;**44**(40):6456-6482. DOI: 10.1002/anie.200462473

[44] Maihom T, Choomwattana S, Wannakao S, Probst M, Limtrakul J. Ethylene epoxidation with nitrous oxide over Fe-BTC metal-organic frameworks: A DFT study. Chemphyschem. 2016;**17**(21):3416-3422. DOI: 10.1002/cphc.201600836

[45] Maihom T, Sawangphruk M, Probst M, Limtrakul J. A computational study of the catalytic aerobic epoxidation of propylene over the coordinatively unsaturated metal-organic framework Fe3(btc)2: Formation of propylene oxide and competing reactions. Physical Chemistry Chemical Physics. 2018;**20**(9):6726-6734. DOI: 10.1039/c7cp07550b

[46] Xiao DJ, Oktawiec J, Milner PJ, Long JR. Pore Environment Effects on Catalytic Cyclohexane Oxidation in Expanded Fe2 (dobdc) Analogues. Journal of the American Chemical Society. 2016;**138**(43):14371-14379. DOI: 10.1021/jacs.6b08417

[47] Zuluaga S, Fuentes-Fernandez EMA, Tan K, Xu F, Li J, Chabal YJ, et al. Understanding and controlling water stability of MOF-74. Journal of Materials Chemistry A. 2016;**4**(14): 5176-5183. DOI: 10.1039/C5TA10416E

[48] Calleja G, Sanz R, Orcajo G, Briones D, Leo P, Martínez F. Copper-based MOF-74 material as effective acid catalyst in Friedel-Crafts acylation of anisole. Catalysis Today. 2014;**227**:130-137

[49] Valvekens P, Vandichel M, Waroquier M, Van Speybroeck V, De Vos D. Metal-dioxidoterephthalate MOFs of the MOF-74 type: Microporous basic catalysts with well-defined active sites. Journal of Catalysis. 2014;**317**:1-10. DOI: 10.1016/j.jcat.2014.06.006

[50] i Xamena FXL, Casanova O, Tailleur RG, Garcia H, Corma A. Metal organic frameworks (MOFs) as catalysts: A combination of Cu2+ and Co2+ MOFs as an efficient catalyst for tetralin oxidation. Journal of Catalysis. 2008;**255**(2):220-227. DOI: 10.1016/j.jcat.2008.02.011

[51] Ryan P, Konstantinov I, Snurr RQ, Broadbelt LJ. DFT investigation of hydroperoxide decomposition over copper and cobalt sites within metal-organic frameworks. Journal of Catalysis. 2012;**286**:95-102. DOI: 10.1016/j.jcat.2011.10.019

[52] Leus K, Vandichel M, Liu YY, Muylaert I, Musschoot J, Pyl S, et al. The coordinatively saturated vanadium MIL-47 as a low leaching heterogeneous catalyst in the oxidation of cyclohexene. Journal of Catalysis. 2012;**285**(1):196-207. DOI: 10.1016/j.jcat.2011.09.014

[53] Vandichel M, Biswas S, Leus K, Paier J, Sauer J, Verstraelen T, et al. Catalytic performance of vanadium MIL-47 and linker-substituted variants in the oxidation of cyclohexene: A combined theoretical and experimental approach. ChemPlusChem. 2014;**79**(8): 1183-1197. DOI: 10.1002/cplu.201402007

[54] Han Y, Li J-R, Xie Y, Guo G. Substitution reactions in metal-organic frameworks and metal-organic polyhedra. Chemical Society Reviews. 2014;**43**(16):5952-5981. DOI: 10.1039/C4CS00033A

[55] Xiao DJ, Bloch ED, Mason JA, Queen WL, Hudson MR, Planas N, et al. Oxidation of ethane to ethanol by N2O in a metal-organic framework with coordinatively unsaturated iron(II) sites. Nature Chemistry. 2014;**6**(7):590-595. DOI: 10.1038/nchem.1956

[56] Verma P, Vogiatzis KD, Planas N, Borycz J, Xiao DJ, Long JR, et al. Mechanism of oxidation of ethane to ethanol at Iron(IV)-oxo sites in magnesium-diluted Fe$_2$(dobdc). Journal of the American Chemical Society. 2015;**137**(17):5770-5781. DOI: 10.1021/jacs.5b00382

[57] Hirao H, Ng WKH, Moeljadi AMP, Bureekaew S. Multiscale model for a metal-organic framework: High-spin rebound mechanism in the reaction of the oxoiron(IV) species of Fe-MOF-74. ACS Catalysis. 2015;**5**(6):3287-3291

[58] Chung LW, Sameera WMC, Ramozzi R, Page AJ, Hatanaka M, Petrova GP, et al. The ONIOM method and its applications. Chemical Reviews. 2015;**115**(12):5678-5796. DOI: 10.1021/acscatal.5b00475

[59] Rappé AK, Casewit CJ, Colwell KS, Goddard WA III, Skiff WM. UFF, a full periodic table force field for molecular mechanics and molecular dynamics simulations. Journal of the American Chemical Society. 1992;**114**(25):10024-10035. DOI: 10.1021/ja00051a040

[60] Liao P, Getman RB, Snurr RQ. Optimizing open iron sites in metal-organic frameworks for ethane oxidation: A first-principles study. ACS Applied Materials & Interfaces. 2017;**9**(39):33484-33492. DOI: 10.1021/acsami.7b02195

[61] Impeng S, Siwaipram S, Bureekaew S, Probst M. Ethane C-H bond actIVation on the Fe(IV)-oxo species in a Zn-based cluster of metal-organic frameworks: A density functional theory study. Physical Chemistry Chemical Physics. 2017;**19**(5):3782-3791. DOI: 10.1039/c6cp07771d

[62] Brozek CK, Dincă M. Ti3+−, V2+/3+−, Cr2+/3+−, Mn2+−, and Fe2+−substituted MOF-5 and redox reactivity in Cr-and Fe-MOF-5. Journal of the American Chemical Society. 2013;**135**(34):12886-12891. DOI: 10.1021/ja4064475

[63] Evans JD, Sumby CJ, Doonan CJ. Post-synthetic metalation of metal-organic frameworks. Chemical Society Reviews. 2014;**43**(16):5933-5951. DOI: 10.1039/C4CS00076E

[64] Brozek CK, Dincă M. Cation exchange at the secondary building units of metal-organic frameworks. Chemical Society Reviews. 2014;**43**(16):5456-5467. DOI: 10.1039/C4CS00002A

[65] Rimoldi M, Bernales V, Borycz J, Vjunov A, Gallington LC, Platero-Prats AE, et al. Atomic layer deposition in a metal-organic framework: Synthesis, characterization, and performance of a solid acid. Chemistry of Materials. 2017;**29**(3):1058-1068. DOI: 10.1021/acs.chemmater.6b03880

[66] Liu T, Vermeulen NA, Howarth AJ, Li P, Sarjeant AA, Hupp JT, et al. Adding to the arsenal of zirconium-based metal-organic frameworks: The topology as a platform for solvent-assisted metal incorporation. European Journal of Inorganic Chemistry. 2016;**2016**(27):4349-4352. DOI: 10.1002/ejic.201600627

[67] Bernales V, Ortuño MA, Truhlar DG, Cramer CJ, Gagliardi L. Computational design of functionalized metal–organic framework nodes for catalysis. ACS Central Science. 2017;**4**(1):5-19. DOI: 10.1021/acscentsci.7b00500

[68] Ortuño MA, Bernales V, Gagliardi L, Cramer CJ. Computational study of first-row transition metals supported on MOF NU-1000 for catalytic acceptorless alcohol dehydrogenation. Journal of Physical Chemistry C. 2016;**120**(43):24697-24705. DOI: 10.1021/acs.jpcc.6b06381

[69] Bernales V, League AB, Li Z, Schweitzer NM, Peters AW, Carlson RK, et al. Computationally guided discovery of a catalytic cobalt-decorated metal-organic framework for ethylene dimerization. Journal of Physical Chemistry C. 2016;**120**(41):23576-23583. DOI: 10.1021/acs.jpcc.6b07362

[70] Li Z, Peters AW, Bernales V, Ortuño MA, Schweitzer NM, Destefano MR, et al. Metalorganic framework supported cobalt catalysts for the oxidative dehydrogenation of propane at low temperature. ACS Central Science. 2017;**3**(1):31-38. DOI: 10.1021/acscentsci.6b00290

[71] Bernales V, Yang D, Yu J, Gümüşlü G, Cramer CJ, Gates BC, et al. Molecular rhodium complexes supported on the metal-oxide-like nodes of metal organic frameworks and on Zeolite HY: Catalysts for ethylene hydrogenation and dimerization. ACS Applied Materials & Interfaces. 2017;**9**(39):33511-33520. DOI: 10.1021/acsami.7b03858